MAUSAM, **65**, 2 (April 2014), 233-244

551.501.777

Observation and numerical simulation of terrain-disrupted wavy motion in the boundary layer with minor temperature inversion/isothermal at the Hong Kong international airport

P. W. CHAN

Hong Kong Observatory, 134A Nathan Road, Kowloon, Hong Kong, China

(*Received 11 June 2012, Modified 3 September 2013*)

e mail : pwchan@hko.gov.hk

सार – इस शोध पत्र में हाँग काँग के अन्तरराष्ट्रीय हवाई अड्डे के मैदानी भूभाग को विघटित करने वाले वायुप्रवाह के न्यून तापमान प्रतिलोमन (1 डिग्री से. से कम) / समताप सहित परिसीमा के स्तर में तरंगित गति को प्रस्तुत किया गया है। 13 अप्रैल 2012 को मिनीसोडार से मापे गए उर्ध्वाधर वेग से मैदानी भूभाग के निकट लगभग 3 मीटर प्रति सैकेंड के तरंग परिमाण देखे गए जिसमें 200 मीटर पर 5 से 6 मीटर प्रति सैकेंड की वृद्धि देखी गई। तरंगित गति का प्रेक्षण प्रकाशीय संसूचन और रेंजिंग (लीडार) प्रणाली से विकिरण वेग के कॉनिकल स्कैन जैसे अन्य मौसम वैज्ञानिक मापों से नहीं लिया गया है। उच्च विभेदन वाले सांख्यिकीय मौसम प्रागुक्ति मॉड़ल का उपयोग करते हुए इसका अध्ययन और अधिक विस्तार से किया गया। मॉड़ल अनुकरण परिणामों से यह पता चला है कि तरंगित गति, पर्वतीय क्षेत्र से लेकर हवाई अड्डे के दक्षिणी भाग द्वारा दक्षिण से दक्षिण-पश्चिम की ओर चलने वाली पवनों के वायु प्रवाह विघटन से संबंधित रहे है।

ABSTRACT. Wavy motion in the boundary layer with minor temperature inversion (less than 1 degree Celsius)/isothermal for terrain-disrupted airflow at the Hong Kong International Airport is documented in the present paper. Wave magnitude of about 3 m/s near the ground increasing to 5 to 6 m/s at 200 m has been observed from the vertical velocity measurement from a minisodar on 13 April, 2012. The wavy motion is not observed from other meteorological measurements, such as conical scan of the radial velocity from a Light Detection And Ranging (LIDAR) system. It is studied in more detail using high-resolution numerical weather prediction model. It is shown in the model simulation results that the wavy motion appears to be associated with airflow disruption of the prevailing south to southwesterly winds by a mountain to the south of the airport.

Key words – LIDAR, Radiometer observations, Minisodar observation.

1. Introduction

The Hong Kong International Airport (HKIA) is situated in an area of complex terrain. To its south is the mountainous Lantau Island with peaks rising to about 1000 m above mean sea level with valleys of 400 m in between. Terrain-disrupted airflow occurs over the airport for background easterly through southeasterly to southwesterly winds. The airflow disturbances are monitored through two-dimensional depiction of the line-of-sight velocities as measured by Doppler Light Detection And Ranging (LIDAR) systems in non-rainy conditions and by Terminal Doppler Weather Radar (TDWR) under rain. However, such instruments mainly measure the distribution of the horizontal wind component over a large area. Examples of the horizontal distribution of radial velocities in terrain-disrupted airflow, such as mountain waves, jets, wakes, etc. could be found in Shun and Chan (2008) as observed by LIDAR measurements.

The vertically profiling, remote-sensing meteorological instruments help depict the variations of the vertical velocity in association with the terrain-disrupted airflow. They include boundary-layer type radar wind profilers and minisodars. The observations by a minisodar in stable stratified boundary layer in the spring time, namely, gravity wave in the lower atmosphere, are documented in Chan (2012a). The minisodar gives basically sinusoidal variation of the vertical velocity over a period of about an hour in association with the wave. The present paper is the first attempt to document similar variation of the vertical velocity as measured by the

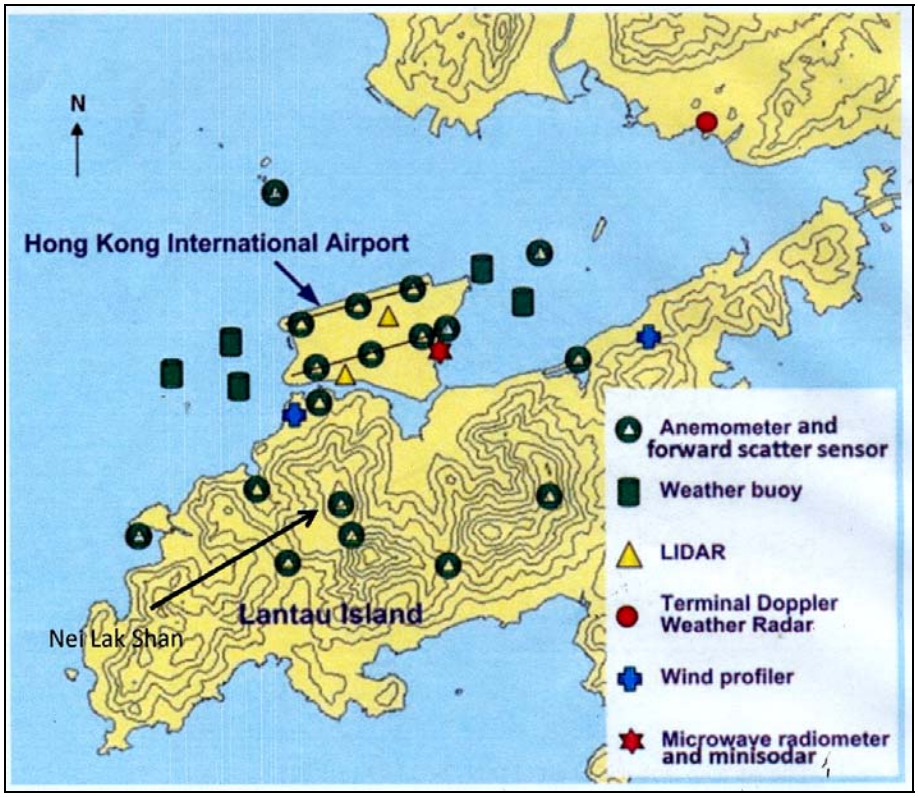

Fig. 1. The meteorological instruments inside and around HKIA. The height contours are in 100 m. The length of each runway I 3,800 m, which could be used as a scale of the figure

minisodar in the boundary layer with minor temperature inversion (less than 1 degree Celsius)/isothermal in late spring/summer at HKIA, and to explain the phenomenon by comparing with the simulation results of a high-resolution numerical weather prediction (NWP) model.

2. Equipment

In the present paper, as far as wind data are concerned, only observations from a LIDAR and a minisodar are described, and some basic information about these two instruments is given here.

There are two Doppler LIDARs operating at HKIA (locations in Fig. 1), each serving one of the two runways of the airport. The LIDAR uses a laser beam with a wavelength of 2 micron to measure the radial velocity over a maximum range of about 10 km. It is configured to scan along the glide paths of the runway corridors in order to detect potential windshear that may be encountered by the arriving/departing aircraft, and the scanning is performed for both directions of each runway (namely, 070 direction to the east-northeast, and 250 direction to the west-southwest). The laser beam is configured to rotate in between these two directions, and in the process of the rotation it provides an overview, conical scan of the radial velocity in the airport area. The results of the conical scan would be given in this paper.

The minisodar under consideration in this paper is situated at the shoreline anemometer site in Fig. 1. It aims at measuring the low-level wind profile to be countered by the aircraft on approach to the south runway from the east/departing from the south runway to the east. It is a monostatic sodar with an acoustic beam of a central frequency of 4500 Hz swinging in three directions in order to measure the three components of the wind. Wind data up to a height of 200 m are collected with a spatial resolution of 5 m. The minisodar has been recently introduced to HKIA and its application for windshear detection in terrain-disrupted airflow is being explored. It has been demonstrated to capture the windshear in low-level easterly jet in spring time, as documented in Chan (2012a).

A ground-based, multi-channel microwave radiometer is also operated at the shoreline anemometer

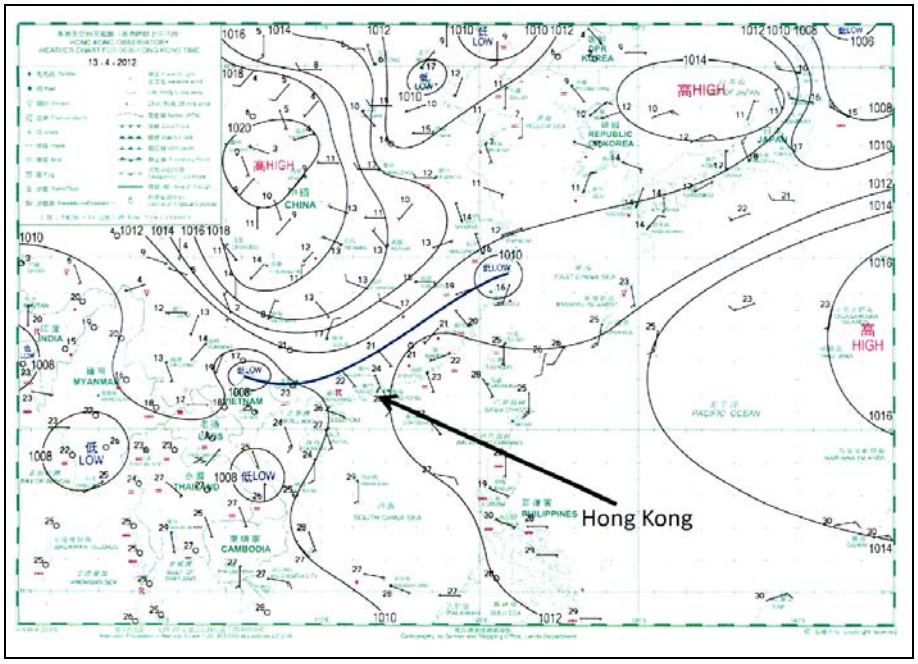

Fig. 2. The surface isobaric chart at 0000 UTC, 13 April, 2012

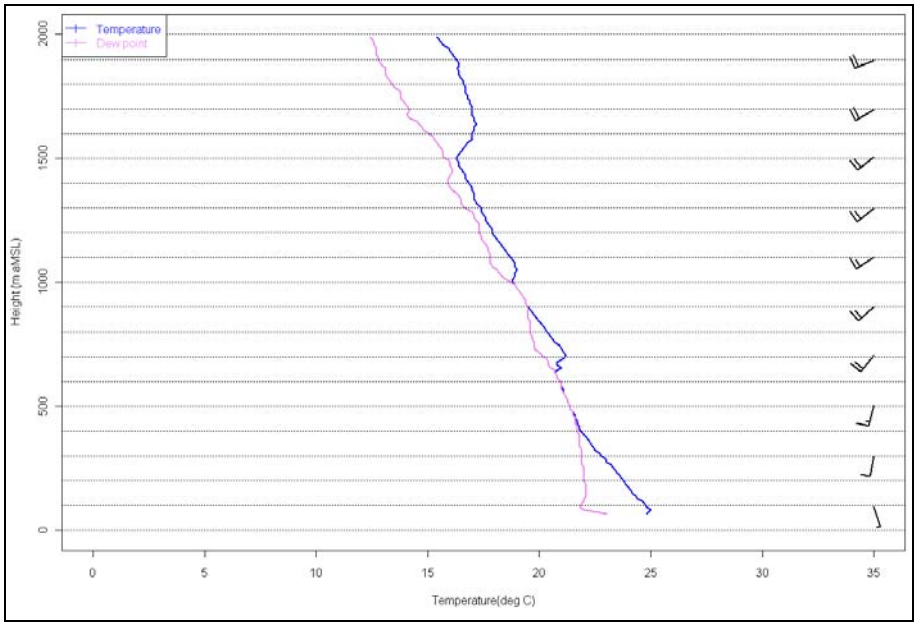

Fig. 3. The wind direction (upper), wind speed (middle) and temperature and dew point (lower) profiles from the radiosonde measurements at King's Park at 0000 UTC, 13 April, 2012

site (Fig. 1). It is used to measure the temperature and relative humidity profiles up to 10 km above ground at the airport. The brightness temperature measurements from 7 oxygen channels and 7 water vapour channels are used in this regard to retrieve the relevant thermodynamic profiles.

3. Synoptic situation

The case under consideration occurs in the morning to early afternoon on 13 April, 2012. The surface isobaric chart at 8 a.m. on that day (0000 UTC, with Hong Kong time = UTC + 8 hours) is shown in Fig. 2. A trough of

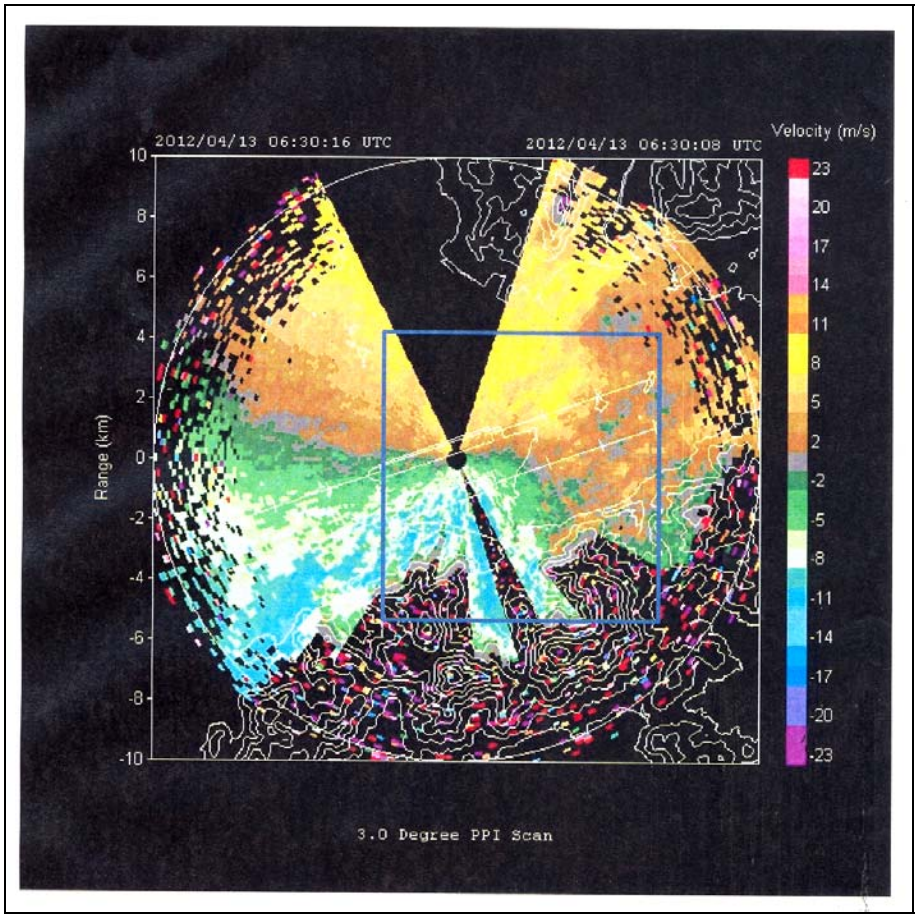

Fig. 4. The conical scan of the radial velocity at an elevation angle of 3 degrees from the north-runway LIDAR at 0630 UTC, 13 April, 2012. To ease comparison with simulation results, the model domain of Fig. 11 and 12 is given as a blue rectangle in the above figure

low pressure appeared in the inland area of southern China. Along the south China coastal area including Hong Kong, there were moderate to fresh south to southwesterly winds within the boundary layer. The isobars are rather slack and the southerly winds are not particularly strong on that day.

Radiosonde measurements in Hong Kong are made twice a day (*i.e.*, 0000 and 1200 UTC) at King's Park, which is located at about 20 km to the east of HKIA in the downtown area. The measurement results at 0000 UTC of 13 April are shown in Fig. 3. The winds were south-southeasterly near the ground, and veered gradually to southwesterly at about 700 m above ground. The wind speed over this range of altitude also increased from a couple of m/s near the ground up to about 10 m/s. The temperature was generally decreasing with height, except for a few minor temperature inversions at base heights of 600, 1000 and 1500 m. The boundary layer was very humid with small dew point depression, as typical in southerly flow originating from the South China Sea in late spring/early summer.

3.1. *LIDAR and radiometer observations*

The radial velocity from the conical scan from the north runway LIDAR with an elevation angle of 3 degrees at 0630 UTC on 13 April, 2012 at HKIA is shown in Fig. 4. It could be seen that south-southwesterly flow prevailed in the airport area, with a maximum wind velocity reaching about 11 m/s. However, probably because of terrain disruption together with sea breeze effect, there were areas of reversed flow (colour green) against the background south-southwesterly flow (coloured yellow and brown) at a few kilometres to the east and northeast of the LIDAR.

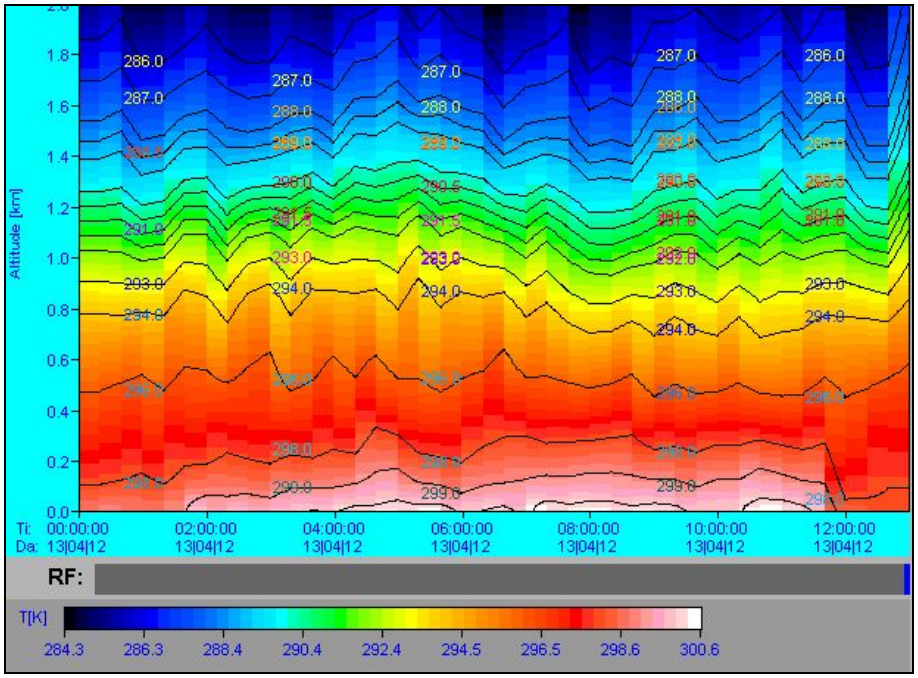

Fig. 5. The boundary-layer temperature from the microwave radiometer between 0000 and 1300 UTC of 13 April, 2012

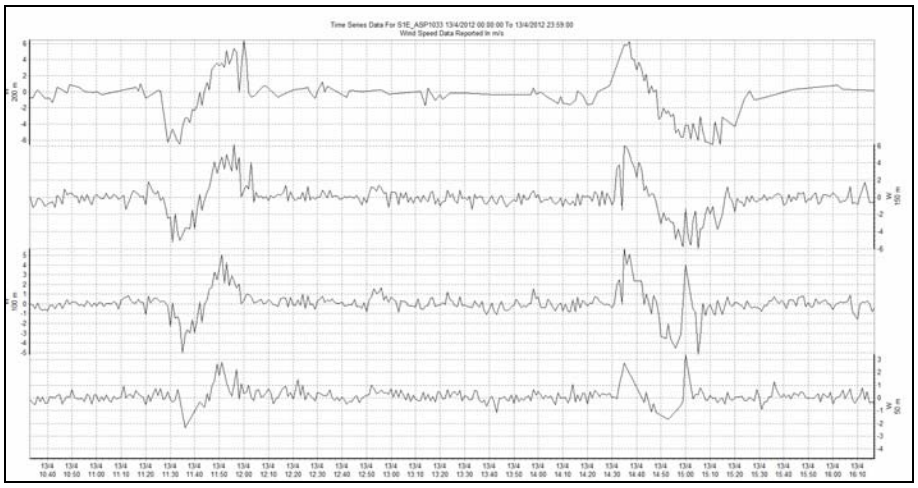

Fig. 6. Time series of vertical velocity at 50, 100, 150 and 200 m (from bottom to top) as measured by the minisodar on 13 April, 2012. The time axis is in Hong Kong time

The time-height display of the boundary-layer temperature profiles as measured by the microwave radiometer is shown in Fig. 5. It could be seen that the temperatures in the lower atmosphere decreased gradually with height throughout the day. At around 0300 UTC, there was a drop of the temperature between 400 and 500 m above ground. Between about 0530 UTC and 0545 UTC, there were temperature drops between 200 and 500 m above ground. Vertical velocity oscillation (described below) was observed after 30 minutes or so from the temperature drop timings. Further study would be required to find out the physical relation between the temperature drops and the vertical velocity oscillation.

3.2. *Minisodar observation*

The minisodar gave moderate to fresh southerly flow at the shoreline anemometer site during the daytime on

(a)

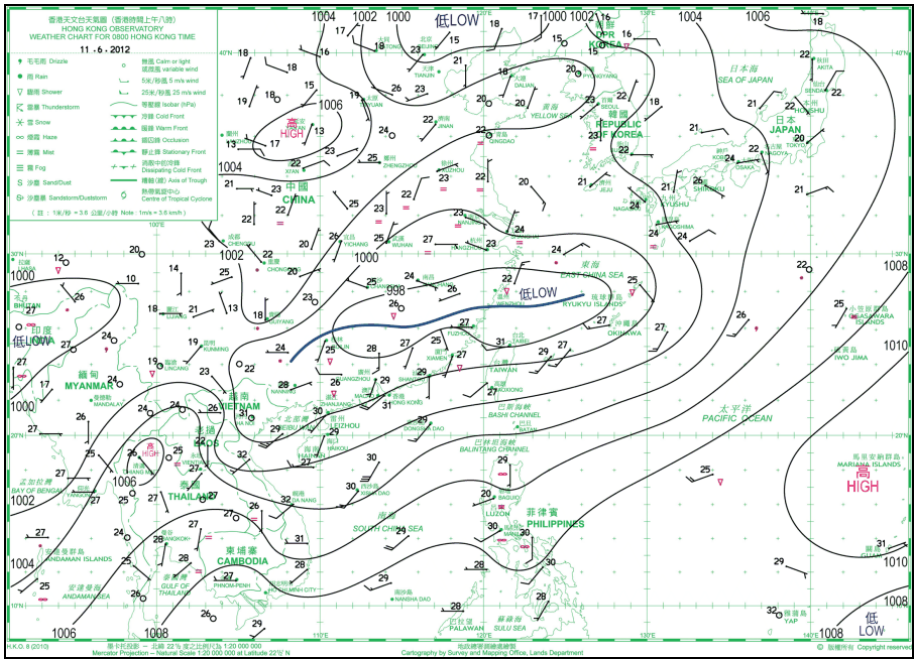

(b)

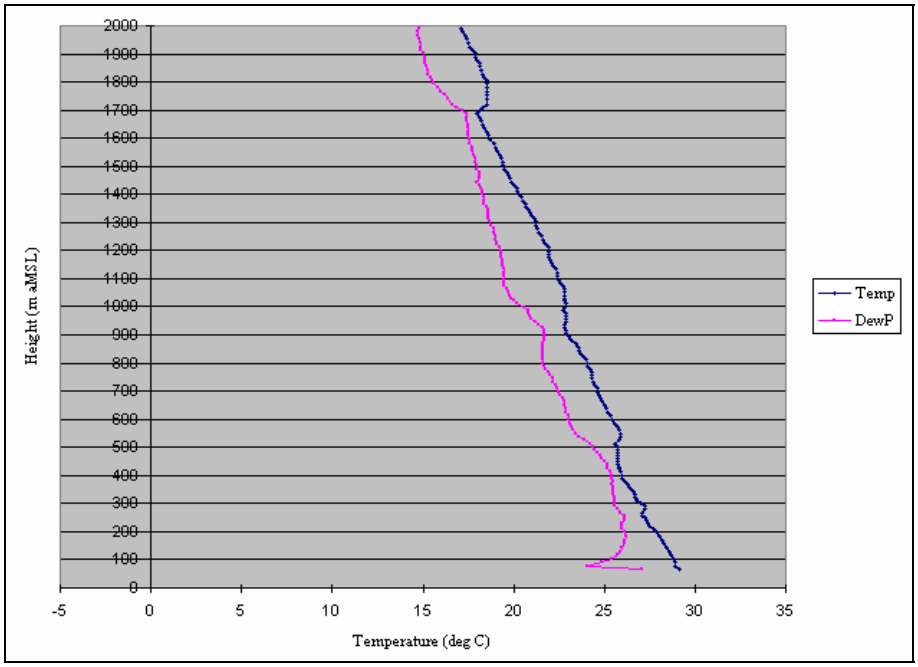

Figs. 7(a&b). The southwesterly case of 11 June, 2012. (a) surface isobaric chart at 8 a.m., (b) radiosonde profiles of temperature and dew point at 8 a.m.

13 April (not shown). On the other hand, the vertical velocity data from this instrument showed some signatures of wavy motion in this period. The time series of vertical velocity at four selected heights is shown in Fig. 6, namely, 50, 100, 150 and 200 m above ground. There are sinusoidal variations of the vertical velocity in two time intervals, namely, between 11:30 a.m. and noon, and between 2:30 and 3:30 p.m. For the latter time interval, there are in fact two sinusoidal variations in the first 100 m above ground, with a longer period for the first variation (about 30 minutes) and a shorter period for the second variation (about 10 minutes). The magnitude of

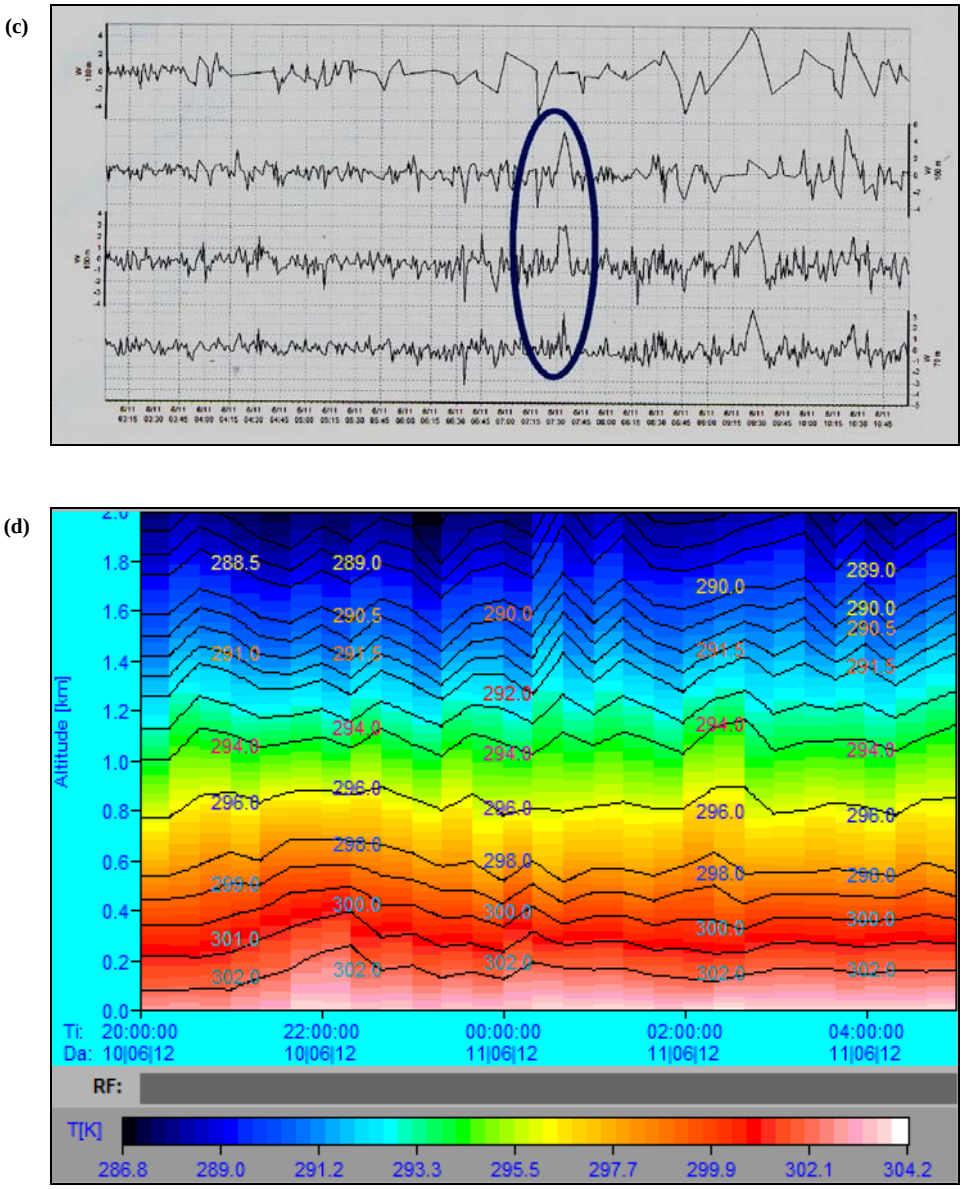

Figs. 7(c&d). The southwesterly case of 11 June, 2012, (c) minisodar's vertical velocity data (time in HKT):wave highlighted in the ellipse and (d) radiometer's temperature data (time in UTC)

the vertical velocity wave is smaller at lower altitude, with a value of 3 m/s at 50 m, and reaches larger value at higher altitude, with a value of 5-6 m/s at 200 m.

Since the lower atmosphere is shown to have at most minor temperature inversion (less than 1 degree Celsius)/isothermal by both the radiosonde and radiometer measurements, the sinusoidal variations in the vertical velocity do not appear to be gravity waves that are normally observed in stably stratified boundary layer at HKIA. The origin of such waves is studied in more detail using simulation results of NWP model. Before getting into the NWP results, we would examine if there is similar wave occurrence at other times of late spring/summer of 2012.

3.3. *Other cases*

In order to see if there are any meteorological parameters which may suggest the occurrence/non-occurrence of waves in southwesterly flow situation, the minisodar database in the period April to July 2012 has

(a)

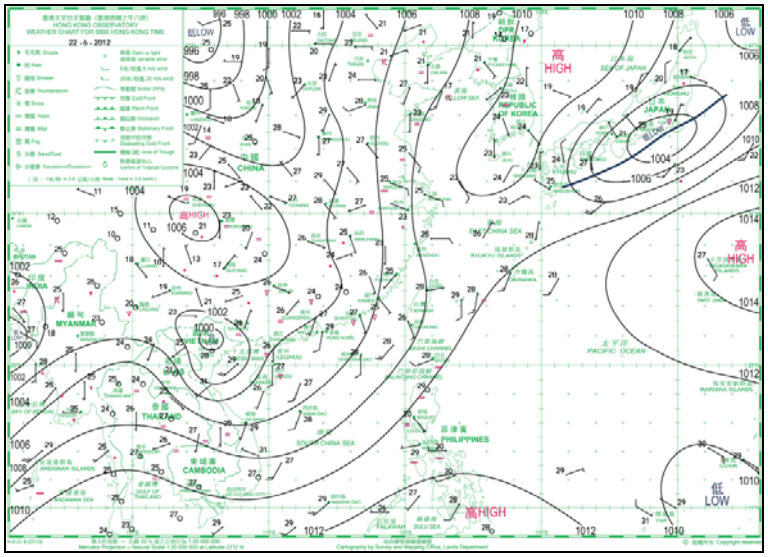

(b)

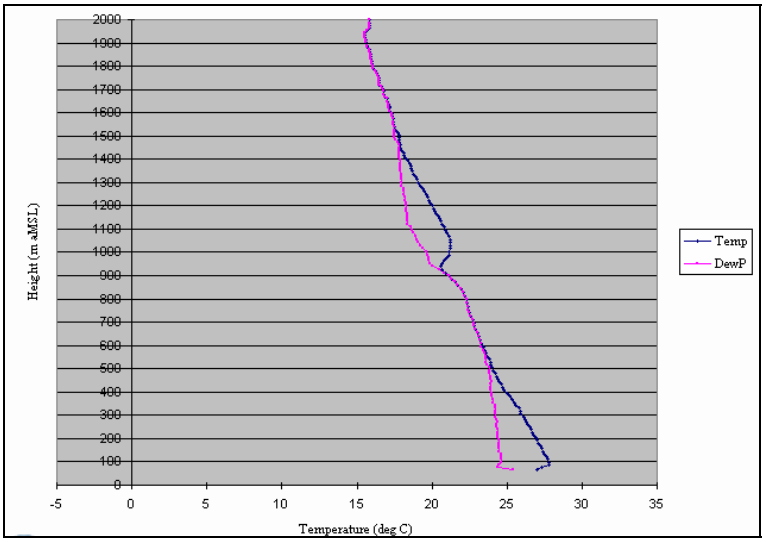

(c)

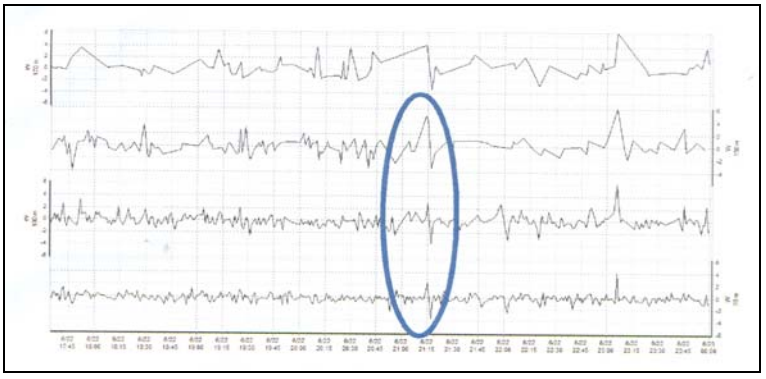

Figs. 8(a-c). The southwesterly case of 22 June 2012, (a) surface isobaric chart at 8 a.m., (b) radiosonde profiles of temperature and dew point at 8 p.m. and (c) minisodar's vertical velocity data (time in HKT): wave highlighted in the ellipse

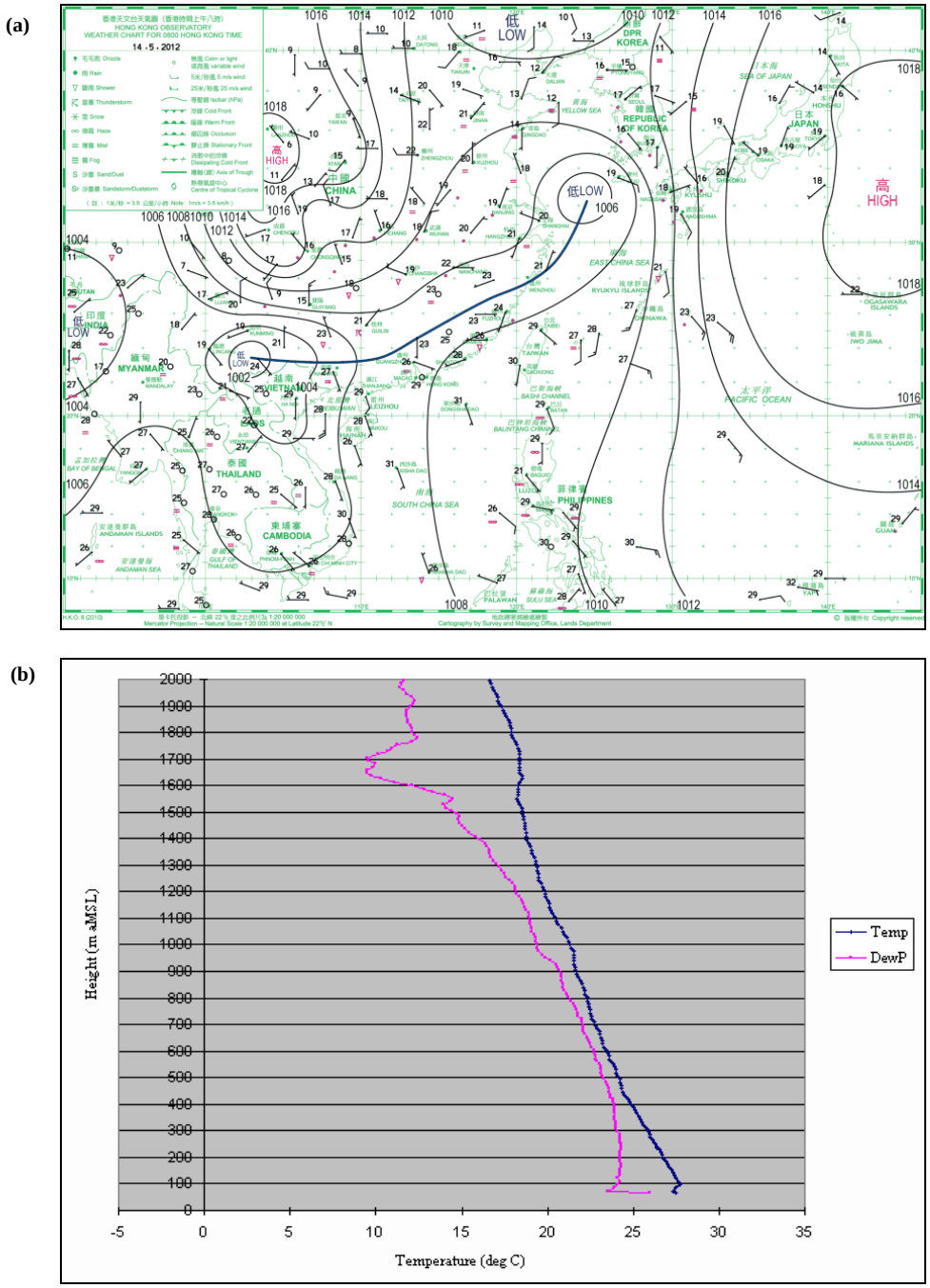

Figs. 9(a&b). The southwesterly case of 14 May 2012. (a) isobaric chart at 8 a.m. and (b) radiosonde's temperature and dew point profiles at 8 a.m.

been searched through. Two more cases of waves could be identified, namely, on 11 June and 22 June 2012, though the magnitudes of the waves are much smaller than that of the case of 13 April 2012. Fig. 7 show the surface isobaric chart, the radiosonde profiles of temperature and dew point, minisodar's vertical velocity data (with the wave highlighted) and radiometer data for the case of 11 June 2012. It could be seen that there are some pressure levels with minor temperature inversions/isothermals within the boundary layer of the atmosphere, namely, at about 300 m, 550 m and between 900 and 1100 m above mean sea level. Boundary layer temperature profiles from the radiometer also show that, at about 6:20 a.m. of 11 June, 2012 (2220 UTC of 10 June, 2012), there is a

(a)

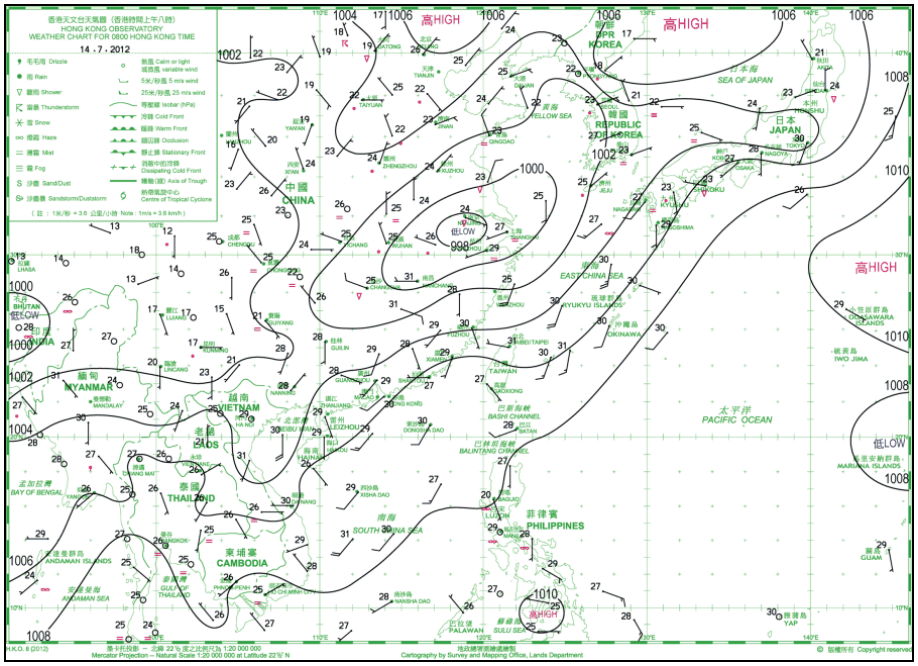

(b)

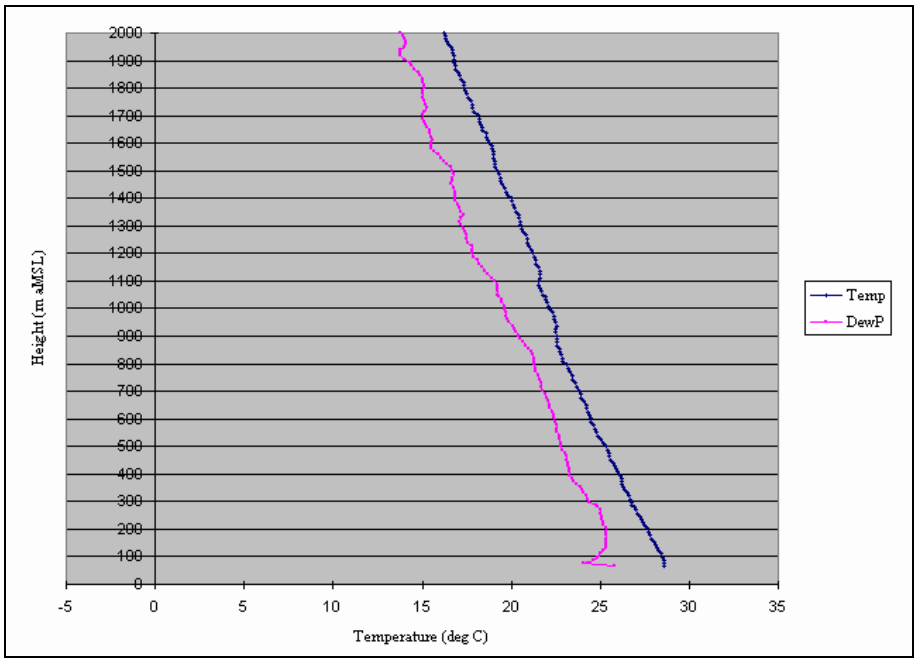

Figs. 10(a&b). The southwesterly case of 14 July 2012, (a) isobaric chart at 8 a.m. and (b) radiosonde's temperature and dew point profiles at 8 a.m.

temperature drop between 100 m and 800 m above ground, before the occurrence of the wave. Figs. 8 (a-c) show the isobaric chart, radiosonde data and minisodar data for the case of 22 June 2012. Unfortunately the radiometer broke down at that time and there were no boundary layer profiles from this instrument. Nonetheless, the radiosonde profile shows minor temperature inversions/isothermals, namely, near the ground and between 900 and 1000 m. As such, based on the observations of a limited number of cases, it appears that minor temperature inversion/isothermal, together with temperature drop within the boundary layer of the atmosphere, may be associated with the occurrence of the wave of vertical velocity.

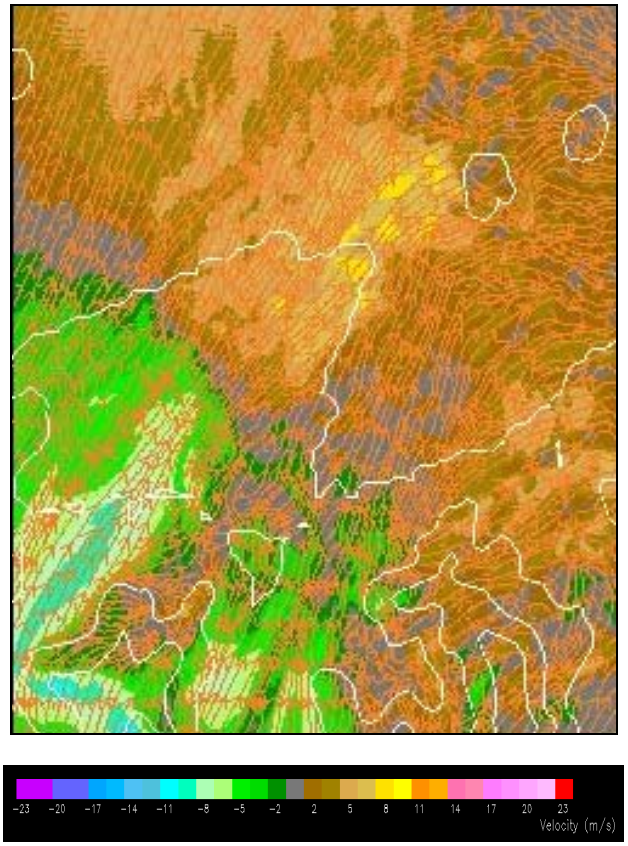

Fig. 11. The simulated radial velocity of the LIDAR at 200 m at 0635 UTC, 13 April 2012. The model simulated wind field is resolved along the measurement radials of the LIDAR to produce the simulated radial velocity

There are far more cases without the occurrence of waves. The meteorological data of two such cases, namely, 14 May 2012 and 14 July 2012, are shown in Figs. 9(a & b) and 10(a & b) respectively. One common feature is the absence of minor temperature inversion/isothermal in the temperature profile in the radiosonde data.

4. NWP simulation results

In order to better resolve the complicated terrain at the airport area, large eddy simulation (LES) is performed with Regional Atmospheric Modelling System (RAMS) version 4.4. More details about the model could be found in Cotton *et al.* (2003). The model setup is the same as that in Chan (2012b). The outer boundary is provided by the Operational Regional Spectral Model (ORSM) of the Hong Kong Observatory at a horizontal resolution of 20 km. It is nested with RAMS with four nesting runs, namely, horizontal resolution of 4 km, 800 m, 200 m and 50 m. Deardorff (1980) turbulence parameterization

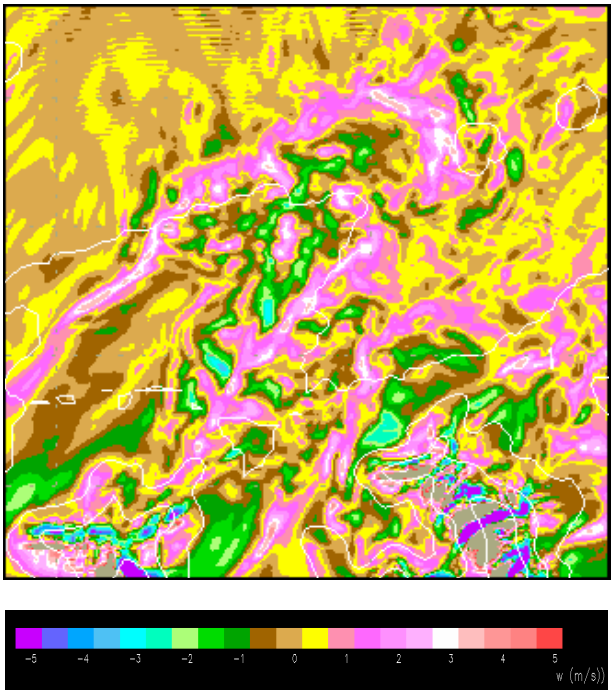

Fig. 12. The simulated vertical velocity at 200 m at 0635 UTC, 13 April, 2012

scheme is used in the latter three nested runs. The model is initialized at 0000 UTC, 13 April, 2012. In the following part of this section, the Figs. 11 and 12 are prepared using the simulation results at the innermost domain, namely, a horizontal resolution of 50 m. The model results with the finest resolution are compared with other measurements, e.g. the LIDAR's radial velocity plot in Fig. 4 (with radial resolution of 100 m). Because of the complexity of the calculation, attempt has not been made to reduce the resolution of the model simulation result to that of the LIDAR for direct comparison.

To validate the model results, the horizontal velocity at a height of 200 m above ground is resolved along the line-of-sights of the north runway LIDAR. This simulated LIDAR radial velocity imagery at 0635 UTC is shown in Fig. 11. It could be seen that the pattern of radial velocity is very similar to the actual observations in Fig. 4. South-southwesterly flow is simulated to prevail in the airport area. On the other hand, near the eastern edge of the model domain, the flow field deviates slightly from this prevailing south-southwesterly flow. Based on the simulated horizontal wind field, it may be concluded that the model forecast is generally consistent with the actual data.

The simulated vertical velocity at a height of 200 m above ground is shown in Fig. 12. Probably arising from

terrain disruption of the prevailing flow, there are waves originating from Nei Lak Shan (location in Fig. 1) and propagating downstream. As a result, at the location of the minisodar, there could be vertical velocity of 3 to 4 m/s. Both upward motion (positive vertical velocity) and downward motion (negative vertical velocity) could be possible. From the NWP simulation results, it appears that the minisodar is picking up some wavy motions originating from the disruption of the prevailing south to southwesterly airflow by Nei Lak Shan on Lantau Island.

5. Conclusion

Wavy motion as demonstrated in the sinusoidal variation of the vertical velocity from a minisodar is documented for the boundary layer with minor temperature inversion/isothermal at HKIA. A number of waves could be identified in the time series of the vertical velocity at a number of altitudes, with a magnitude of 3 m/s near the ground to 5 to 6 m/s at 200 m. Such waves are not evident from the wind measurements from other remote-sensing meteorological instruments at HKIA, such as the radial velocities from the LIDAR. They are studied in more detail using high-resolution NWP model. The simulation results could reproduce the general flow pattern at the airport area, and suggest that the waves are associated with terrain-disrupted airflow from a tall mountain to the south of the airport. This is the first attempt to document and explain wavy motion at HKIA in the boundary layer with minor temperature inversion/isothermal using vertical velocity measurements from a ground-based instrument and high-resolution NWP model. The climatology of such waves could be studied with the accumulation of more observations.

References

Chan, 2012a, "An observational study of gravity waves associated with a shallow easterly airstream at the Hong Kong International Airport using remote-sensing meteorological instruments", to appear in Weather.

Chan, 2012b, "A significant wind shear event leading to aircraft diversion at the Hong Kong international airport", *Meteorological Applications*, **19**, 10-16.

Cotton, W. R., Pielke Sr, R. A., Walko, R. L., Liston, G. E., Tremback, C., Jiang, H., McAnelly, R. L., Harrington, J. Y., Nicholls, M. E., Carrio, G. G. and McFadden, J. P., 2003, "RAMS 2001: Current status and future directions", *Meteor. Atmos. Phys*., **82**, 5-29.

Deardorff, J. W., 1980, "Stratocumulus-capped mixed layers derived from a three-dimensional model", *Bound-Layer Meteor*., **18**, 495-527.

Shun, C. M. and Chan, P.W., 2008, "Applications of an infrared Doppler LIDAR in detection of windshear", *Journal of Atmospheric and Oceanic Technology*, **25**, 637-655.